Advances in Bioscience and Biotechnology, 2010, 1, 185-189 **ABB**
doi:10.4236/abb.2010.13026 Published Online August 2010 (http://www.SciRP.org/journal/abb/)

Structure and properties of bone-like-nanohydroxyapatite/ gelatin/polyvinyl alcohol composites[#]

Feng Wang[1*], Enyan Guo[1], Enmin Song[2], Ping Zhao[1], Jinhua Liu[1]

[1]Shandong Key Laboratory of Glass and Ceramics, Shandong Institute of Light Industry, Jinan, China;
[2]Coal Industry Design and Research Corporation Limited, Jinan, China.
Email: wf890916@163.com

Received 14 April 2010; revised 7 May 2010; accepted 8 May 2010.

ABSTRACT

Bone-like nanohydroxyapatite powders (b-nanoHA) were synthesized in simulated body fluid (SBF). The b-nanoHA, gelatin (Gel) and Polyvinyl Alcohol (PVA) were used to prepare bone-like composites (b-nanoHA/ Gel/PVA) at room temperature. Characterizations of b-nanoHA powders and b-nanoHA/Gel/PVA composites were investigated by using X-ray diffraction (XRD), transmission electron microscopy (TEM), High-resolution transmission electron microscopy (HRTEM), scanning electron microscopy (SEM) and Fourier transform infrared spectroscopy (FT-IR). Bending strength and compressive strength of the composite were tested. It was found that microstructure of the b-nanoHA powders was whisker shape and its crystalline degree was low similar to natural bone, bending strength and compressive strength of the b-nanoHA/Gel/PVA composite depended on the mixing ratio of HA, Gel and PVA, and also PVA could induce the network formation in the b-nanoHA/Gel/ PVA composite.

Keywords: SBF; b-nanoHA/Gel Composites; Structure; Mechanical Strength; Cross-Linkage

1. INTRODUCTION

Inorganic bioceramic hydroxyapatite (HA), being the main inorganic composition of the hard tissues in natural bones, has been extensively studied for medical application due to its excellent bioactivity and biocompatibility [1-3]. However, pure HA is low fracture toughness and low degradation properties limiting its clinic application in hard tissue bones [4,5]. In order to solve these shortcomings, collagen, the main organic component of nature bone, is well used to prepare bone-like composites of collagen and HA. Gelatin, being a hydrolysate of collagen, recently is also studied to substitute the expensive collagen. Many kinds of HA/ Gel composites were produced and their properties were investigated [6-9].

The dimensions and morphology of HA crystals in bone affects its mechanical properties [10]. It has been found that their length, width and thichness are almost in the range of nano-size [11]. Therefore, the studies of nano-HA/Gel composites have been received extensive attention.

To improve the mechanical properties, various kinds of aldehyde were used as cross-linkage in nano-HA/Gel composites [12-14]. It is known that the composites are limited to apply in bone reconstruction due to toxic aldehyde. In recent years, HA/PVA/Gel composite was prepared by some investigators [15-17].

In this paper, in order to repair the material similar to natural bone, the bone-like nanohydroxyapatite powders (b-nanoHA) was synthesized in simulated body fluid (SBF). The b-nanoHA, Gel and PVA were used to prepare bone-like composites (b-nanoHA/Gel/PVA) at room temperature. The characters of the b-nanoHA powders, the b-nanoHA/Gel and the b-nanoHA/Gel/ PVA composites were studied.

2. MATERIAL AND METHODS

2.1. Production of Powders and Composites

SBF[18,19] was prepared by dissolving NaCl, $NaHCO_3$, KCl, $K_2HPO_4{\cdot}3H_2O$, $MgCl_2{\cdot}6H_2O$, $CaCl_2$ and Na_2SO_4 in deionized water. Reagent was added (amount of each reagent given in **Table 1**), one by one after each reagent was completely dissolved in 2000 ml of deionized water, in the order given above. The concentration of prepared SBF is given in **Table 2**. A measured amount of $CaCl_2$ (1.946 g) and $K_2HPO_4{\cdot}3H_2O$ (1.596 g) was added to the prepared SBF solution, under continuous stirring, to produce suspension, according to the following reaction:

$$14K_2HPO_4{\cdot}3H_2O + 14CaCl_2 \rightarrow$$
$$HA + 4Ca(H_2PO_4)_2 + 28KCl + 50H_2O$$

Then the suspension was transferred into a glass bottle

[#] Sponsor: Natural Science Foundation of Shandong Province, China (Y2007F33)

Table 1. Amount of each reagent.

Reagent	NaCl	$NaHCO_3$	KCl	$K_2HPO_4{\cdot}3H_2O$	$MgCl_2{\cdot}6H_2O$	$CaCl_2$	Na_2SO_4
Amount (g)	15.992	0.700	0.448	0.456	0.610	0.556	0.142

Table 2. Ion concentrations of SBF solution.

Ion	Na^+	Cl^-	HCO_3^-	K^+	Mg^{2+}	Ca^{2+}	HPO_4^{2-}	SO_4^{2-}
Concentration(mM)	142.0	147.8	4.2	5.0	1.5	2.5	1.0	0.5

and was tightly sealed. The bottle was kept at 37˚C in a water bath for 72 hours. The resulting suspension was filtrated and washed several times with deionized water, then the HA slurry was obtained as a precursor to prepare the b-nanoHA/Gel and the b-nanoHA/Gel/PVA composites. On the other hand, HA slurry was dried at 50˚C for 24 h, the b-nanoHA powders were obtained.

Commercial gelatin (molecular weight 50000-250000) was produced in Shanghai Chemical Reagent Company. The Gel was completely dissolved at 40˚C in deionized water. The commercial PVA (molecular weight 75000-79000) was produced in Shanghai Chemical Reagent Company. The PVA was completely dissolved at 80˚C in deionized water. The mixing ratio of HA, Gel and PVA was changed to prepared a series composite samples. Composites were shaped by using homemade cylindrical dies 8 mm in diameter and 25 mm in length. The shaped composites were placed at air for 24 h, then dried at 50˚C in air drier for 72 h. Due to water loss, each dried sample was about 5 mm in diameter and 20 mm in length. The experiment schematic diagram for preparing the b-nanoHA/Gel/PVA composite is shown as **Figure 1**.

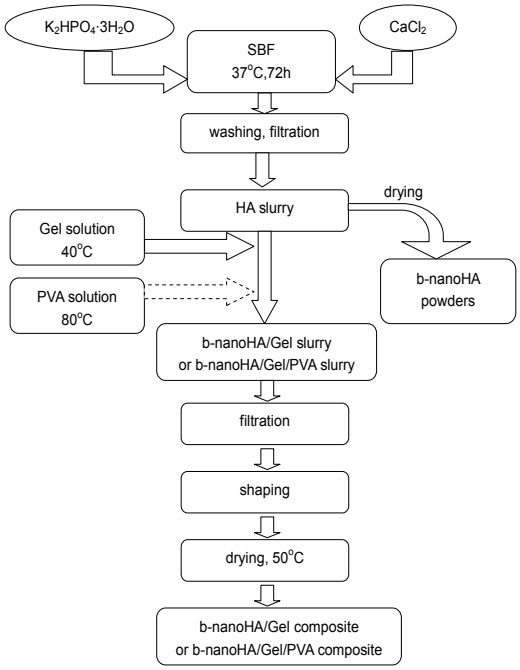

Figure 1. Experimental schematics for preparing the b-nanoHA powders, b-nanoHA/Gel composites and b-nanoHA/Gel/PVA composites.

2.2. Testing Methods

The prepared samples were studied by XRD (Model: D-Max, Rigaku Co., Tokyo, Japan) at the step size of 0.02˚ (2 θ) and the speed of 10˚ (2 θ) per min. A Cu K α tube operated at 40 Kv and 80 mA was used for the generation of X-rays. Morphological and sizes of the b-nanoHA powders were investigated by HRTEM (model: Philips Tecnai20U-TWIN). Microstructure characterization of cross-sections of the composites was observed by SEM (model: Quanta200) and by TEM (model: H800). Three point bending strength and compressive strength of composites were measured by universal testing machine (model: RG D-5), at a cross-head of 0.5 mm/min with a span of 15 mm for the samples of Φ5 mm × 20 mm and at a head of 1 mm/min for the samples of Φ5 mm × 10 mm, respectively. B-nanoHA/Gel/PVA powders were obtained by pulverizing and used in FT-IR (model: Nicolet Nexus470).

3. RESULTS AND DISCUSSION

3.1. XRD

Figure 2 is the X-ray diffraction spectra of PVA, Gel,

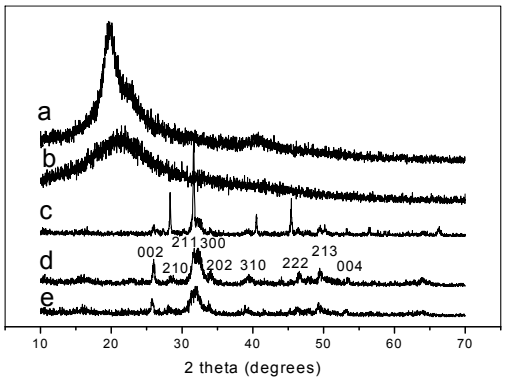

Figure 2. XRD spectra of the samples. (a) PVA; (b) Gel; (c) b-nanoHA powders; (d) b-nanoHA/Gel composite; (e) b-nano HA/Gel/PVA composite.

b-nanoHA powders, b-nanoHA/Gel composite (mass ratio, HA:Gel = 6:4) and b-nanoHA/Gel/PVA composite (mass ratio, HA:Gel:PVA = 6:4:2). From the **Figure 2(a)**,

the X-ray diffraction peak shape of PVA was broad at θ = 19.8˚, as well as its peak shows that PVA was non-crystal structure. The X-ray diffraction peak shape of Gel in **Figure 2(b)** was similar to PVA, non-crystal structure. The X-ray diffraction peak of b-nanoHA powders in **Figure 2(c)** were good match with the JCPDS (09-0432) standard. In **Figure 2(d)** and **Figure 2(e)**, the X-ray diffraction spectra of b-nanoHA/Gel composite and b-nanoHA/ Gel/PVA composite were very similar to that of b-nano HA powders, but their diffraction peak broadening was stronger than pure b-nanoHA powders, due to organic gelatin and organic PVA being introduced. Some studies [20] have shown that human bone apatite is of diffraction peak broadening in XRD spectra.

3.2. Morphology Analysis

The morphology and size of b-nanoHA powders under HRTEM was shown in **Figure 3**. It can be seen that b-nanoHA powders was composed of a large number of long and straight HA whiskers being of 3-6 nm in diameter and 50-120 nm in length. During high-magnification HRTEM observation (**Figure 3(b)**), it was found that the HA whiskers were very unstable under strong electron beam irradiation. After about 10 seconds of electron irradiation, the edges of the whiskers became irregular or even disappear.

SEM photographs of the cross-section of b-nanoHA/ Gel (HA:Gel = 6:4) composite and b-nanoHA/Gel/PVA (HA:Gel:PVA = 6:4:2) were shown in **Figure 4(a)** and **Figure 4(b)**. It is apparent that distribution of b-nanoHA powders, gelatin and PVA in the composite was very uniform. The more high-magnification SEM photographs of the cross-sections of b-nanoHA/Gel composite and b-nanoHA/Gel/PVA composite were not obtained due to the composites unstable by electron irradiation under high-magnification SEM.

From the TEM photographs, the microstructures of b-nanoHA/Gel composite (HA:Gel = 6:4) and b-nano HA/Gel/ PVA (HA:Gel:PVA = 6:4:2) were observed, as shown in **Figure 5(a)** and **Figure 5(b)**. Organic-inorganic interaction among gelatin, PVA and HA was very uniform. The size of HA whiskers in composites was similar to HA powders, about 50-150 nm in length. **Figure 5** also shows the corresponding SAED pattern for the two composites. It was a typical micrograph for HA/ Gel nano-composite [21], being of the small spots and diffused ring pattern, indicting the existence of low degree crystalline nano-phase.

3.3. Mechanical Property Analysis

Bending strength and compressive strength of five samples were provided in **Table 3**, each datum was the average value of six samples with the same mass ratio

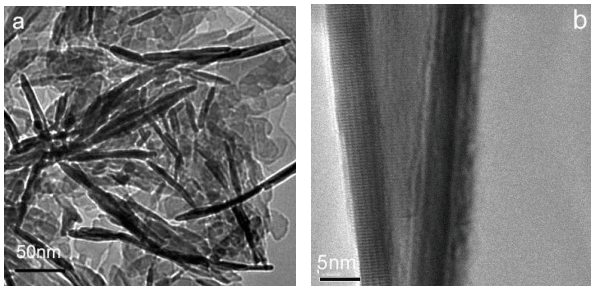

Figure 3. HRTEM images of b-nanoHA powders. (a) low-magnification HRTEM image; (b) high-magnification HRTEM image.

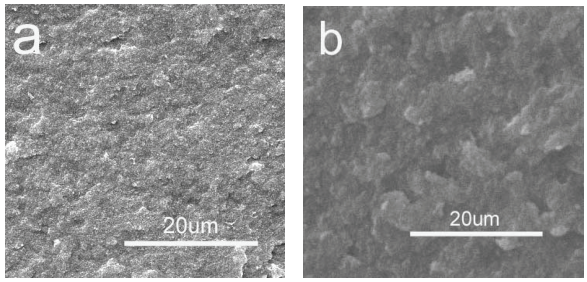

Figure 4. SEM photographs of the cross-sections of composites. (a) b-nanoHA/Gel composite (HA:Gel = 6:4); (b) b-nano HA/Gel/PVA composite (HA:Gel:PVA = 6:4:2).

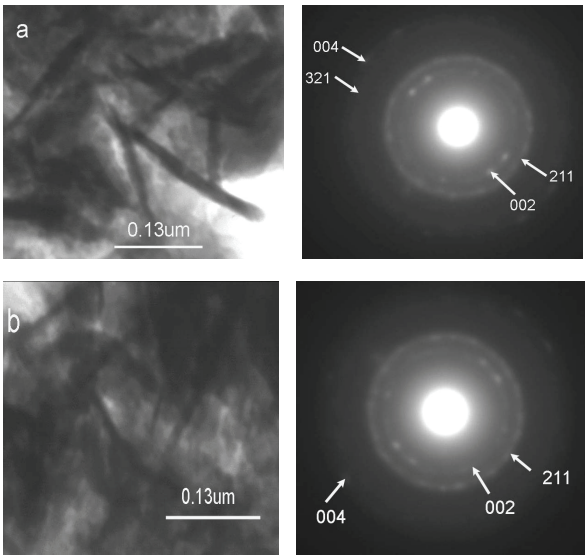

Figure 5. TEM photographs of composites. (a) b-nanoHA/Gel composite (HA:Gel = 6:4) and corresponding SAED pattern; (b) b-nanoHA/Gel/PVA composite (HA:Gel:PVA = 6:4:2) and corresponding SAED pattern.

(HA:Gel). It is seen that, with Gel content increasing, both bending strength and compressive strength of b-nanoHA/Gel composites increase initially, and decrease when the ratio of HA to Gel is more than 6:4. The values of bending strength and compressive strength of

Table 3. Bending strength and compressive strength of b-nanoHA/gel composites.

Order	Mass ratio	Bending strength (MPa)	Compressive strength （MPa）
Sample 1	HA:Gel = 8:2	16.83	10.79
Sample 2	HA:Gel = 7:3	19.06	19.82
Sample 3	HA:Gel = 6:4	35.97	39.20
Sample 4	HA:Gel = 5:5	22.38	29.77
Sample 5	HA:Gel = 4:6	18.35	17.06

Table 4. Bending strength and compressive strength of b-nanoHA/gel/PVA composites.

Order	Mass ratio	Bending strength (MPa)	Compressive strength （MPa）
Sample 6	HA:Gel = 6:4:1	36.22	39.73
Sample 7	HA:Gel = 6:4:2	58.11	60.21
Sample 8	HA:Gel = 6:4:3	49.79	52.17

sample 3 were the highest among the five samples, 35.97 MPa and 39.20 MPa, respectively.

Table 4 showed bending strength and compressive strength of three samples, each datum was the average value of five samples with the same mass ratio (HA: Gel:PVA). It is observed that bending strength and compressive strength of b-nanoHA/Gel/PVA composites are higher than those of b-nanoHA/Gel composites. Moreover, the values of bending strength and compressive strength of sample 7 being the highest, 58.11 MPa and 60.21 MPa, respectively, are higher than some reports [15,16]. It is thought that PVA has cross-linking effect in b-nanoHA/Gel/PVA composites.

3.4. FT-IR

Figure 6(a) showed chemical bond positions for the reference sample PVA, such as C-H stretching and bending at 2945 cm^{-1} and 1337 cm^{-1}, C-C stretching at 854 cm^{-1}, O-H stretching at 3328 cm^{-1}, C-O stretching at 1098 cm^{-1} and CH-OH bending at 1427 cm^{-1}. From **Figure 6(b)**, the spectral intensity of O-H stretching at 3328 cm^{-1} was stronger than that of PVA in **Figure 6(a)** due to HA containing abundance of OH^- ions. It is suggested that new chemical bonds were not formed between HA and PVA in the HA/PVA composite because the bond frequencies (3328 cm^{-1}, 1427 cm^{-1}) being relate to OH were not changed. **Figure 6(c)** showed typical amide bond frequencies for the reference sample Gel, such as amide A at 3419 cm^{-1} for N-H stretching, amide I at 1659 cm^{-1} for C=O stretching, amide II at 1537 cm^{-1} for N-H bending and amide III at 1240 cm^{-1} for C-N stretching. From

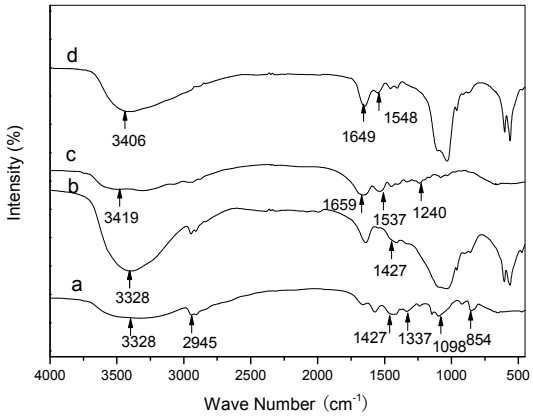

Figure 6. FT-IR spectra for samples. (a) PVA; (b) HA + PVA; (c) Gel; (d) HA + Gel.

Figure 6(d), the spectral feature of all amide bonds was obviously changed, such as the band frequencies of amide A and amide I were blue-shifted to 3406 cm^{-1} and 1649 cm^{-1}, respectively, of amide II was red-shifted to 1548 cm^{-1} and of amide III disappeared. From the spectral change of the amide bonds between the reference Gel and the HA/Gel composite, it is indicated that the inorganic-organic (Ca^{2+}-COO^-) bonds were formed in the HA/Gel composite [9,21].

Figure 7 is FT-IR spectra of HA/Gel/PVA composites. It is observed that the band frequencies of amide A and amide I were blue-shifted, of amide II was red-shifted. From the spectral change of the amide bands, it is indicated that the hydrogen bond (OH···NH) was formed between the active group OH in PVA and the group NH in Gel. On the other hand, we can observe the intensity of C-H bond became stronger with the amount of PVA increasing. The optimal amount of PVA in HA/Gel/PVA composites was HA:Gel:PVA = 6:4:2 (mass ratio) in the range of experiments, corresponding to the mechanical

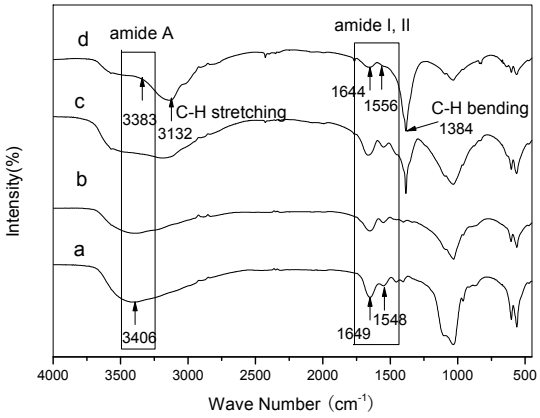

Figure 7. FT-IR spectra for samples. (a) HA:Gel = 6:4 composite; (b) HA:Gel:PVA = 6:4:1 composite; (c) HA:Gel:PVA = 6:4:2 composite; (d) HA:Gel:PVA = 6:4:3 composite.

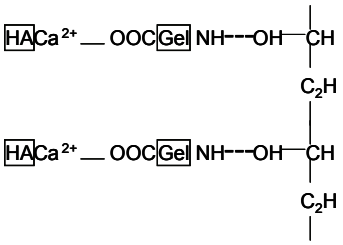

Figure 8. Sketch map of the complex net-structure in HA/Gel/PVA composites (____coordination bond, ---hydrogen bond).

property analysis above.

From the above analysis for **Figure 6** and **Figure 7**, it is considered that there was a complex network structure in HA/Gel/PVA composites, being existence of Ca^{2+}-COO^- bond between HA and Gel, and being OH···NH bond between Gel and PVA. **Figure 8** is the sketch map of the complex network structure in HA/Gel/PVA composites. It is thought that PVA could be a good kind of cross-linkage in HA/Gel/PVA composites or other bone substitution materials.

4. CONCLUSIONS

Diameter and length of HA synthesized in SBF are almost in the range of nano-size and its crystalline is low similar to natural bone. The mechanical properties of b-nanoHA/Gel/PVA composites depended on the mass ratio of HA, Gel and PVA. The highest values of bending strength and compressive strength appeared when mass ratio was HA:Gel:PVA = 6:4:2 in the range of experiments. PVA might be a potential cross-linkage instead of toxic aldehyde in the field of preparing artificial bone.

REFERENCES

[1] Hench, L.L. (1991) Bioceramics: From concept to clinic. *Journal of America Ceramic Society*, **74(7)**, 1487-1510.

[2] Larry, L.H. (1998) Biomaterials: A forecast for the future. *Biomaterials*, **19(16)**, 1419-1423.

[3] Koutsopoulos, S. (2002) Synthesis and characterization of hydroxyapatite crystals: A review study on the analytical methods. *Journal of Biomedical Materials Research*, **62(4)**, 600-612.

[4] Weiner, S. and PRICE, P. (1986) Disaggregation of bone into crystals. *Calcified Tissue International*, **39(5)**, 365-375.

[5] Salyer, K.E. and Hall, C.D. (1989) Porous hydroxyapatite as an only bone graft substitute for maxillofocid surgery. *Plast Reconstructive Surgery*, **84**, 236-244.

[6] Bakoš, D., Soldán, M. and Hernández-Fuentes, I. (1999) Hydroxyapatite-collagen-hyaluronic acid composite. *Biomaterials*, **20(2)**, 191-195.

[7] Chang, M.C., Ko, C.C. and Douglas, W.H. (2003) Preparation of hydroxyapatite-gelatin nanocomposite. *Biomaterials*, **24(17)**, 2853-2862.

[8] Chang, M.C. and Douglas, W.H. (2007) Cross-linkage of hydroxyapatite/gelatin nanocomposite using imide-based zero-length cross-linker. *Journal of Materials Science*: *Materials in Medicine*, **18(10)**, 2045-2051.

[9] Chang, M.C. (2008) Organic-inorganic interaction between hydroxyapatite and gelatin with the aging of gelatin in aqueous phosphoric acid solution. *Journal of Materials Science*: *Materials in Medicine*, **19(11)**, 3411-3418.

[10] Fratzl, P., Groschner, M., Vogl, G., Plenk, H., Jr., Eschberger, J., Fratzl-zelman, N., Koller, K. and Klaushofer, K. (1992) Mineral crystals in calcified tissues—A comparative study by SAXS. *Journal of Bone Mineral Research*, **7(3)**, 329-334.

[11] Su, X., Sun, K., Cui, F.Z. and Landis, W.J. (2003) Organization of apatite crystals in human woven bone. *Bone*, **32(2)**, 150-162.

[12] Lin, X.Y., Li, X.D., Fan, H.S., Xiao, Y.M., Lu, J. and Zhang X.D. (2005) Comparative investigation of copre -cipitation and in-situ synthesis of nanohydroxyapatite/collagen composite. *Key Engineering Materials*, **284-286**, 839-842.

[13] Charulatha, V. and Rajaram, A. (2003) Influence of different crosslinking treatments on the physical properties of collagen membranes. *Biomaterials*, **24(5)**, 759-767.

[14] Gilberto, G., Elcio, M., Rosemary, A.C.M., Rafael, C.C.L., Daniela, C.J.C. and Wanda, Maria de C. (1999) Biocompatibility studies of anionic collagen membranes with different degree of glutaraldehyde cross-linking. *Biomaterials*, **20(1)**, 27-34.

[15] Wang, M., Li, Y., Xu, F., Zhou, G. and Cheng, L. (2007) Synthesis and characterization of n-HA/PVA/Gel composite. *Key Engineering Materials*, **330-332**, 471-474.

[16] Chang, M.C. (2005) Modification of hydroxyapatite/gelatin composite by polyvinylalcohol. *Journal of Materials Science Letters*, **40(2)**, 505-509.

[17] Suprabha, N. and Arvind, S. (2004) Systematic evolution of a porous hydroxyapatite-poly(vinylalcohol)-gelatin composite. *Colloids and Surfaces B*: *Biointerfaces*, **35(1)**, 29-32.

[18] Viitala, R., Simola, J., Peltola, T., Rahiala, H., Linden, M., Langlet, M. and Rosenholm, J.B. (2000) In vitro bioactivity of aerosol-gel deposited TiO_2 thin coatings. *Journal of Biomedical Materials Research*, **54(1)**, 109-114.

[19] Cüneyt, T.A. (2000) Synthesis of biomimetic Ca-hydroxyapatite powders at 37°C in synthetic body fluids. *Biomaterials*, **21(14)**, 1429-1438.

[20] Carlström, D. and Glas, J.E. (1959) The size and shape of the apatite crystallites in bone as determined from line-broadening measurements on oriented specimens. *Biochimica et Biophysica Acta*, **35**, 46-53.

[21] Chang, M.C., Ko, C.C. and Douglas, W.H. (2003) Conformational change of hydroxyapatite/gelatin nanocomposite by glutaraldehyde. *Biomaterials*, **24(18)**, 3087-3094.

